

Integration–segregation dynamics in functional networks of individuals diagnosed with schizophrenia

Sergio Iglesias-Parro¹  | Juan Ruiz de Miras² | Maria Felipa Soriano³ | Antonio J. Ibáñez-Molina¹

¹Department of Psychology, University of Jaén, Jaén, Spain

²Department of Software Engineering, University of Granada, Granada, Spain

³Mental Health Unit, San Agustín Hospital de Linares, Linares, Spain

Correspondence

Sergio Iglesias-Parro, Department of Psychology, University of Jaén, Jaén, Spain.

Email: siglesia@ujaen.es

Funding information

This research was funded by Agencia Estatal de Investigación, AEI, PID2019-105145RB-I00.

Edited by: John Foxe

Abstract

Schizophrenia has been associated with dysfunction in information integration/segregation dynamics. One of the neural networks whose role has been most investigated in schizophrenia is the default mode network (DMN). In this study, we have explored the possible alteration of integration and segregation dynamics in individuals diagnosed with schizophrenia with respect to healthy controls, based on the study of the topological properties of the graphs derived from the functional connectivity between the nodes of the DMN in the resting state. Our results indicate that the patients show a diminution of the modularity of the DMN and a higher global efficiency, in sparse graphs. Our data emphasise the interest in studying temporal changes in network measures and are compatible with the hypothesis of randomization of functional networks in schizophrenia.

KEYWORDS

EEG, healthy control, integration, schizophrenia, segregation

1 | INTRODUCTION

Schizophrenia (SCZ) is a complex, chronic mental illness characterized by a series of symptoms, including positive (e.g., hallucinations and delusions), negative (e.g., diminished emotional expression and avolition) and cognitive symptoms (e.g., disorganized speech, thought and/or attention). Even today, the causes of schizophrenia remain subject of debate and research. Nevertheless, it has been proposed that the pathophysiology of schizophrenia may be associated with dysfunctional patterns of

integration/segregation in distributed neural networks, rather than with the disruption of the function within any specific structure (Friston & Frith, 1995; Wang et al., 2015; Zhou et al., 2007).

One of the neural networks whose possible dysfunction has been frequently associated with diagnosis of SCZ is the default mode network (DMN). The DMN is a large-scale network that involves association cortex and paralimbic regions but spare sensory and motor cortex, located along the midline of the prefrontal cortex, encompassing the rostral anterior cingulate cortex, posterior cingulate cortex and precuneus (Buckner et al., 2008). It has been proposed that this network is responsible for mental simulations that are used adaptively in internally oriented tasks

Abbreviation: BEM, boundary element method; DMN, default mode network; EEG, electroencephalogram; HC, healthy controls; ICA, independent component analysis; SCZ, schizophrenia.

This is an open access article under the terms of the [Creative Commons Attribution-NonCommercial-NoDerivs](https://creativecommons.org/licenses/by-nc-nd/4.0/) License, which permits use and distribution in any medium, provided the original work is properly cited, the use is non-commercial and no modifications or adaptations are made.

© 2023 The Authors. *European Journal of Neuroscience* published by Federation of European Neuroscience Societies and John Wiley & Sons Ltd.

(Buckner, 2013; Spreng et al., 2009). The activation of the DMN is anti-correlated with the activity of brain networks responsible for external information processing (Bressler & Menon, 2010). Thus, in passive tasks where the experimenter's requirements are minimized, the DMN is more active, and the activity in the areas of the cortex responsible for sensory processing is reduced (Uddin et al., 2009). Likewise, it has been observed that the DMN shows a lower activation during the performance of cognitive tasks than in the resting state or in tasks that require internal concentration (van Buuren et al., 2012).

DMN alterations have been associated with various symptoms of schizophrenia, including positive (Rotarska-Jagiela et al., 2010), negative (Wang et al., 2015) and cognitive symptoms (Zhou et al., 2016). Individuals with an SCZ diagnosis have a diminished capacity to deactivate DMN during task performance (van Buuren et al., 2012; Whitfield-Gabrieli et al., 2009; Whitfield-Gabrieli & Ford, 2012) and elevated DMN resting-state functional connectivity (Liu et al., 2012; Shim et al., 2010; Skudlarski et al., 2010; Whitfield-Gabrieli et al., 2009). However, the results are not univocal, and some studies report decreased low-frequency resting-state functional connectivity within the DMN (Hilland et al., 2022) or widespread decreased connectivity including the DMN (Liang et al., 2006).

The idea of coordination dynamics proposes that the tendency of brain regions to express their specialized functions (segregation) coexists with tendencies to coordinate globally for multiple functions (integration) and that this integration/segregation balance may have an evolutionary function (Deco et al., 2015). In this sense, some authors have proposed that an imbalance in integration/segregation capacity may be related to schizophrenia (Friston et al., 1995; Hu et al., 2017; Liang et al., 2006). The present work aims to explore the possible alteration of integration and segregation dynamics in individuals with an SCZ diagnosis with respect to healthy controls (HC), based on the study of the topological properties of graphs derived from the functional connectivity between the nodes of the DMN in resting state. We start from the assumption that the brain can be understood as a complex network, and we use graph theory as a conceptual framework for studying the topological features of these networks.

Previous graph-theoretical research in SCZ and other psychiatric disorders has demonstrated a disrupted balance between segregation and integration within the functional brain networks. Thus, Rubinov et al. (2009), analyzing weighted graphs, found that the group of individuals with an SCZ diagnosis displayed lower clustering (an indicator of segregation) and shorter path lengths

(an indicator of integration) in comparison to the HC group. Likewise, Vértes et al. (2012) found that topological properties of clustering and modularity (i.e., segregation) were somewhat reduced in childhood-onset SCZ-diagnosed individuals. Studying the topological properties of functional brain networks, (Lynall et al., 2010; Rubinov et al., 2009) found that they were less hierarchical, less small-world, less clustered and less efficiently wired in individuals with an SCZ diagnosis. Comparing HC and individuals with an SCZ diagnosis, (Bassett et al., 2008) found reduced hierarchy and increased connection distance in SCZ, and (Liu et al., 2008) found that individuals with an SCZ diagnosis exhibited lower clustering and lower path length than HC, but no differences were found between groups in efficiency. During a two-back working memory task, Micheloyannis et al. (2006) found that individuals with an SCZ diagnosis did not show small-world properties for alpha, beta and gamma electroencephalogram (EEG) frequency bands.

All these works show the benefits of graph theory to characterize functionally complex networks. However, most of them are focused on the study of the brain system as a whole (e.g., Bassett et al., 2008; Rubinov et al., 2009) or, at most, on the characterization of interregional functional relationships (e.g., Liu et al., 2008). Very few include, specifically, the study of functional connectivity within the DMN. On the other hand, although most of the cited works take advantage of the high spatial resolution provided by fMRI, however, this high temporal resolution is at the cost of lower temporal resolution. Furthermore, fMRI measures activation-related hemodynamics rather than neuronal activity in itself (Bullmore & Sporns, 2009). Finally, most of these papers offer a stationary view of the functional relationships between network communities, as they tend to calculate functional relationships from measures based on averages of the recordings. For these reasons, in the present work, we will use EEG resting state recordings to compare the dynamical topological properties of the DMN in patients with SCZ and HC.

Specifically, we want to compare the dynamics of integration (global efficiency) and segregation (modularity) of the DMN in SC patients and HC. To this end (see Figure 1, for a detailed workflow), we proceeded to record the EEG of individuals with an SCZ diagnosis and HC during 161 s of resting state. We then performed the reconstruction of the cortical sources, which we subsequently parceled into the 14 DMN regions using the Desikan–Killiany atlas (Desikan et al., 2006). For each of these regions and for each subject, using a sliding window system, we obtained 798 correlation matrices,

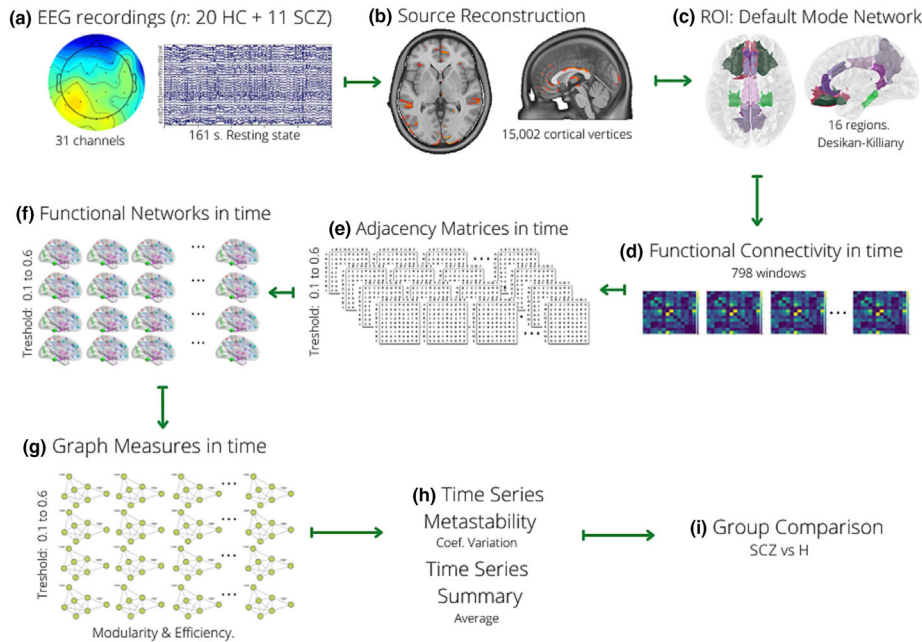


FIGURE 1 Principal steps in the workflow. (a) EEG measurement in HC and SCZ. (b) Source modeling. (c) Parcellation of the default mode network. (d) We calculate with correlation coefficient the functional connectivity in time (798 matrices). (e) Binarize the matrices with thresholds from 0.1 to 0.6. (f) We construct the functional networks (in time, one for each matrix and at each threshold). (g) We obtain for each matrix and at each threshold, network measurements: modularity and global efficiency. (h) Characterize the dynamics of the series as well as stationary measures. (i) Between-group comparisons. EEG, electroencephalogram; HC, healthy controls; SCZ, schizophrenia; ROI, region of interest.

corresponding to each one of the 798 sliding windows, that we binarized using various thresholds (from 0.1 to 0.6). From each of these functional networks over time, we obtained modularity and overall efficiency. For each time series of these two measures (global efficiency and modularity) that reportedly map integration and segregation, respectively, we calculated the coefficient of variation and the mean and then proceeded to compare them between groups.

2 | METHODS

2.1 | Participants

The sample of this study consisted of a group of individuals with an SCZ diagnosis and a group of healthy controls. The group of individuals with an SCZ diagnosis (hereinafter referred to as the SCZ group) consisted of 11 participants who were recruited at the Hospital Universitario San Agustín (Linares, Jaén). The inclusion criteria for participation were an ICD-10 diagnosis of schizophrenia (F20), psychotic disorder (F23) or schizophrenic disorder (F25). The participant's diagnosis was made by the unit psychologist. The mean age of this group was 36.27 years ($SD = 10.28$ years; $min = 23$,

$max = 53$). Out of all the participants, two (18.18%) were women. All participants were dexterous. Regarding the educational level of the participants, two had primary education, eight had secondary education and one had higher education. Regarding the medication, all participants were receiving antipsychotic medication (all atypical). In addition to antipsychotics, one of the participants was receiving antidepressants. Due to differences in active principles, doses and administration methods, we converted the doses of all antipsychotics into chlorpromazine equivalents ($M = 818.18$ mg, $SD = 407.75$ mg).

Twenty participants in the control group (hereinafter referred to as the HC group) were recruited from the students of the University of Jaén, the staff of the University St. Agustin Hospital of Linares (Jaén) and an Adult School of Linares (Jaén). The average age of this group was 40.72 years ($SD = 11.96$ years; $min = 23$, $max = 57$). Out of all participants, seven (35%) were women. Only two participants were left-handed. Regarding the educational level of the participants, one had primary education, 12 had secondary education and seven had higher education. There was no significant association between sex and group ($\chi^2 [1, N = 31] = 0.97, p = 0.32$) or between group and education level ($\chi^2 [2, N = 31] = 3.29, p = 0.19$). The

groups did not differ significantly with respect to age ($t[29] = 1.03$, $p = 0.30$).

For both groups, the exclusion criteria were either a concurrent diagnosis of neurological disorder, a concurrent diagnosis of substance abuse disorder, a history of developmental disability, an inability to sign informed consent, vision disorders (vision disorders that, although corrected with surgery, glasses or contact lenses, result in a loss of visual acuity, e.g., cataracts) or hearing disorders (unless corrected with hearing aids or surgery). In addition, an exclusion criterion for the control group was the diagnosis of a mental disorder (as reported verbally by the participants). All participants gave written informed consent in accordance with the Declaration of Helsinki, and the Jaén Research Ethics Committee approved the study.

The Spanish version (Peralta & Cuesta, 1994) of the Positive and Negative Syndrome Scale (PANSS, Kay et al., 1989) was used to assess psychopathology. PANSS consists of 30 items that evaluate schizophrenic syndrome, and each item is scored according to a scale of 7 degrees of intensity or severity, where 1 is equivalent to the absence of the symptom and 7 to the presence with severity. PANSS can be divided into three subscales: the positive subscale of 7 items ($M = 13.95$, $SD = 4.5$), the negative subscale of 7 items ($M = 19.27$, $SD = 8.18$), and the general psychopathology subscale of 16 items that evaluates the presence of other symptoms in the patient (depression, anxiety and disorientation, among others) ($M = 29.36$, $SD = 7.06$).

2.2 | EEG acquisition

EEG data were acquired while the participants were instructed to rest with their eyes open and look at a stationary cross on a monitor. An active electrode cap (actiCAP™) was used to acquire data from the international 10–20 system of 32 scalp sites. All electrodes were referenced to both mastoids. Electrode impedance was kept lower than 5 k Ω . The EEG data were collected for 161 s at a rate of 500 Hz through a BrainAmps™ amplifier. Data processing was performed with the Brain Vision Analyzer software EEGLAB (Delorme & Makeig, 2004) and MATLAB custom scripts. We applied a bandpass filter with cut-off frequencies of 0.5 and 30 Hz. Blinks and other artefacts were extracted using infomax independent component analysis (ICA) (Bell & Sejnowski, 1995). ICA components with artefacts were selected via visual inspection of the scalp topography, power spectra and raw activity from all components. Once all noisy components were selected, they were eliminated from the original signals.

2.3 | Source reconstruction

A source model consisting of 15,002 current dipoles was used to calculate Kernel inversion matrices for each subject with sLORETA implemented in Brainstorm (Pascual-Marqui, 2002). As an MRI template, we used the ICBM152 brain, distributed with the Brainstorm package. Dipole orientations were constrained normal to the cortex. Using the boundary element method (BEM) as implemented in the OpenMEEG model (Corsi et al., 2020; Kybic et al., 2005), the forward EEG model was computed for each subject. We used the identity matrix as the noise covariance matrix.

2.4 | Parcellation

The source model was then anatomically parcellated using the Desikan–Killiany atlas (Desikan et al., 2006) available in Brainstorm, as no individual anatomies of the participants were available. Automated parcellation by this method has been shown to be comparable to manual labelling (Fischl et al., 2004). According to this parceling scheme, the DMN was defined as the following 14 regions of interest (ROIs): Isthmus cingulate L, Isthmus cingulate R, Lateral orbito frontal L, Lateral orbito frontal R, Medial orbito frontal L, Medial orbito frontal R, Parahippocampal L, Parahippocampal R, Posterior cingulate L, Posterior cingulate R, Precuneus L, Precuneus R, Rostral anterior cingulate L and Rostral anterior cingulate R (where L stands for left and R for right).

2.5 | Functional connectivity

We calculated the Spearman correlation coefficient between the 14 nodes of the DMN that we obtained after parcellation. To take advantage of the temporal resolution of the EEG recordings and thus be able to explore the temporal dynamics of integration and segregation in the DMN, we used a sliding window of 2000 ms with a 90% of overlap on each step and obtained a total of 798 functional connectivity matrices for each participant. The duration of the time series to which we applied the sliding window was 161 s.

The topological properties of the networks obtained after binarizing the matrix of interregional correlations will depend on the choice of the threshold value. In this sense, if the threshold is high and the resulting number of edges is low, the network will be poorly connected and some regional nodes may be disconnected. On the other hand, if the threshold is low, and the number of edges is

high, the network will be more densely connected but will also have a random topology (Bassett et al., 2008). Following the recommendation of Rubinov and Sporns (2010) that networks should ideally be characterized across a broad range of thresholds, in this paper, we used thresholds from 0.1 to 0.6 in steps of 0.1. Thresholds of 0.1–0.6 produce networks limited to 90–40% of the 120 possible edges in a fully connected network of 14 nodes. Following Su et al. (2015), we have selected this range of costs because they cover the spectrum of meaningful networks for resting state data. Thus, we obtained a total of 798 binary matrices (unweighted and undirected) for each of the six thresholds explored. In this study, we removed negative connections from the network to avoid interference (Murphy & Fox, 2017; Rubinov & Sporns, 2010).

2.6 | Graph measures

For each binary graph, at each threshold level, we calculate the global efficiency and the network modularity. The graph measures were calculated with the Brain Connectivity Toolbox, a MATLAB toolbox developed by (Rubinov & Sporns, 2010). These data, anonymized, are stored in Figshare (DOI: [10.6084/m9.figshare.21975899](https://doi.org/10.6084/m9.figshare.21975899)) and also the scripts (DOI: [10.6084/m9.figshare.21990005](https://doi.org/10.6084/m9.figshare.21990005)). Both will be available upon reasoned request.

According to Rubinov and Sporns (2010), the functional segregation metrics capture the ability of a network to perform specialized processing. The presence of clusters in functional networks is interpreted as an indication of segregated neural processing. In this paper, we will measure network segregation using modularity. Modules in networks correspond to clusters of nodes that are internally strongly coupled but externally only weakly coupled (Sporns & Betzel, 2016). According to Simon (1962), modularity is a distinctive characteristic of complex systems, and the importance of modular brain networks in shaping brain dynamics has been identified as a powerful incentive to empirically study changes in brain modularity in mental disorders (Fornito et al., 2015). Heuristically, modularity compares the number of edges inside a cluster with the expected number of edges that one would find in the cluster if the network were a random network (with the same number of nodes, but randomly attached). According to Newman and Girvan (2003), modularity can be quantified by the following expression:

$$Q = \frac{1}{2E} \sum_{ij} (A_{ij} - e_{ij}) \delta(m_i, m_j).$$

where A_{ij} is the ij element of the adjacency matrix of the graph G (the connection status between i and j : $A_{ij} = 1$ when link ij exists; $A_{ij} = 0$, otherwise), e_{ij} is the fraction of edges in the network that connect vertices in the same community and $\delta(m_i, m_j)$ is the Kronecker delta function and equals 1 if nodes i and j belong to the same module (i.e., $m_i = m_j$) and 0 otherwise.

On the other hand, the integration metrics capture the ability to rapidly combine specialized information from distributed brain regions. In this work, we selected global efficiency as the measure of network integration. A larger global efficiency value of the brain network represents a higher information transmission efficiency and a higher integration degree of the brain network. In functional brain networks, global efficiency is inversely related to the topological distance between nodes (the path length) and provides a measure of the overall capacity for parallel information transfer and integrated processing among distributed components of the system with the advantage over the average path length that it can be calculated in disconnected networks (Bullmore & Sporns, 2012; Latora & Marchiori, 2001). The network can be represented as a graph $G(N, M)$ with N nodes and M edges. The global efficiency is defined as follows:

$$E_{glob} = \frac{1}{N(N-1)} \sum_{j \neq i \in G} \frac{1}{l_{ij}}$$

where l_{ij} is the mean of the shortest path length (the average number of steps along the shortest paths for all possible pairs of network nodes) between nodes i and j . For an undirected graph of N nodes, the mean of the shortest path length is as follows:

$$l_{ij} = \frac{1}{N(N-1)} \sum_{j \neq i \in G} d_{ij}$$

where d_{ij} is the length of the shortest path between nodes i and j .

For a more technical description of graph-based metrics frequently used in brain networks, see Bullmore and Sporns (2009) and Rubinov and Sporns (2010). A graphic representation of these concepts can be found in Figure 2.

3 | DATA ANALYSIS AND RESULTS

From the binary graphs, we obtained the dependent variables (efficiency and modularity) both static and

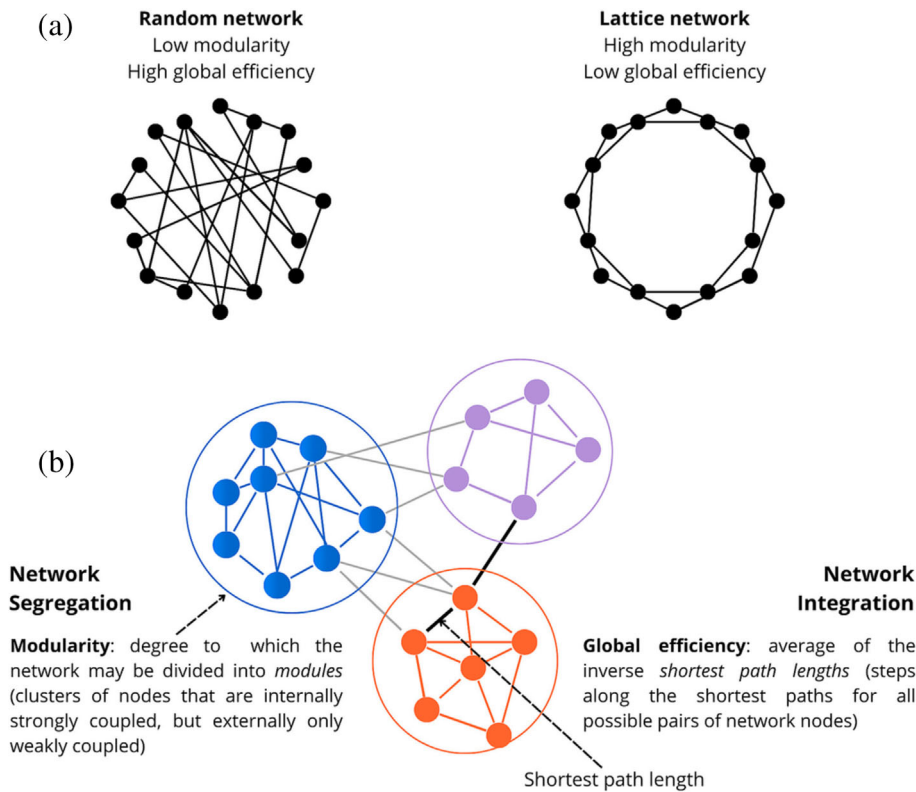


FIGURE 2 Network topologies and graph measures. (a) Network topology examples: Random networks, with randomly determined connections, have high global efficiency, as shown by the many connections crossing the center of the graph, and low modularity, as shown by the relatively few connections between nearby nodes. Lattice networks show the reverse pattern. (b) A simulated network is used to illustrate common terms in network analysis. Nodes are represented as circles, and edges are represented as lines.

dynamic. These data were analyzed using mixed-effects analysis of variance with, group, threshold and their interaction as fixed factors and participants as random factors. Analyses were performed in R using the `lmer()` function of the `lme4` package (Bates et al., 2015). Post hoc comparisons and interaction analyses were made using `emmeans` package (Lenth, 2021). To control the error type I due to the number of comparisons we used the *fdr* procedure (Benjamini & Yekutieli, 2001).

3.1 | Dynamic measures

In order to study the temporal dynamics of modularity and efficiency, for both metrics we calculated the variation coefficient (VC), and these data were summited to a mixed model with intercept as a random factor and group and threshold as fixed factors. The VC allows to compare the variability of the series independently of the means of each group.

The results of the coefficient of variation of modularity (see Figure 3) showed a significant effect for group ($F[1,31] = 5.25; p = 0.02$), a significant effect for threshold ($F[5155] = 9.64; p < 0.01$) and a significant effect for the interaction ($F[5155] = 2.29; p = 0.04$). Pairwise comparisons over the interaction revealed that for threshold values of 0.6, the variability in modularity was significantly higher ($t[199] = 3.80; p < 0.01$)

for HC ($M = 98.6, SD = 111.0$) than for SCZ ($M = 36.5, SD = 36.3$).

The results of the coefficient of variation of efficiency (see Figure 4) showed a significant effect for threshold ($F[5155] = 3.85; p < 0.01$). No significant effect for group ($F[1,31] < 1$) neither for the interaction ($F[5155] = 1.03, p = 0.39$) was found. Post hoc comparisons showed the following significant differences in VC depending on threshold: T1 < T3 ($t[145] = 3.39, p < 0.01$), T1 < T4 ($t[145] = 2.95, p < 0.01$), T2 < T3 ($t[145] = 2.32, p = 0.02$) and T6 < T4 ($t[145] = -2.41, p = 0.01$). Significant contrasts are shown in Table 1.

3.2 | Stationary measures

We also calculated the means across all time windows of modularity and efficiency and these data were summited to a mixed model with intercept as a random factor and group and threshold as fixed factors.

The results of the mean of modularity (see Figure 5) showed a significant effect for group ($F[1,31] = 7.43; p = 0.01$) and a significant effect for threshold ($F[5155] = 27.69; p < 0.01$), but no significant effect was found for the interaction ($F[5155] = 2.25; p = 0.051$). Post hoc comparisons showed the mean of modularity was significantly ($t[33.1] = 2.63; p = 0.01$) higher for the HC group ($M = 0.99, SD = 0.02$) than for the SCZ group

FIGURE 3 Main effects and interaction for the coefficient of variation of modularity depending on group and threshold. (a) Interaction group by threshold. (b) Main effect of group. (c) Main effect of threshold. SCZ, schizophrenia; VC, variation coefficient.

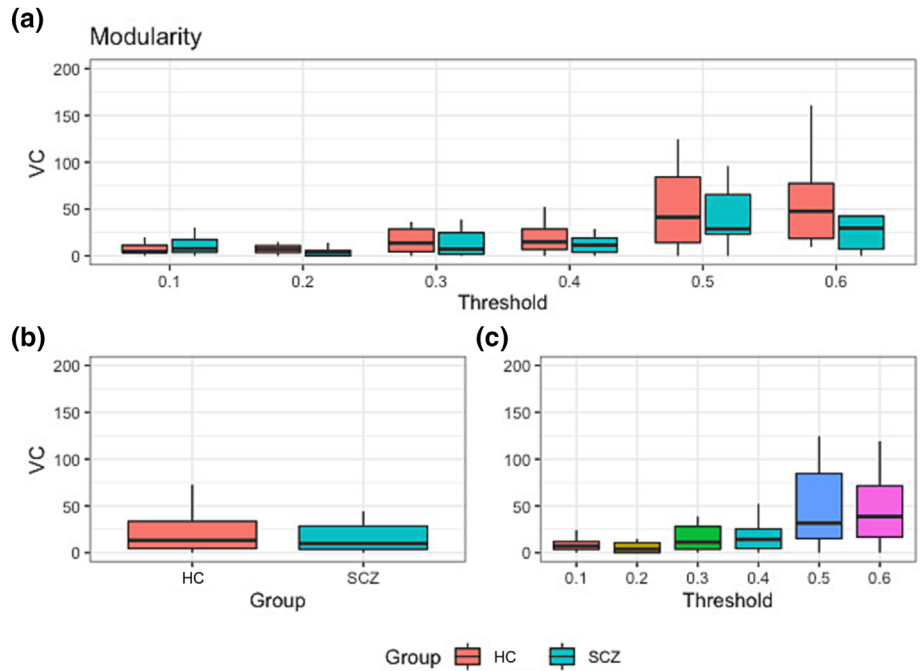
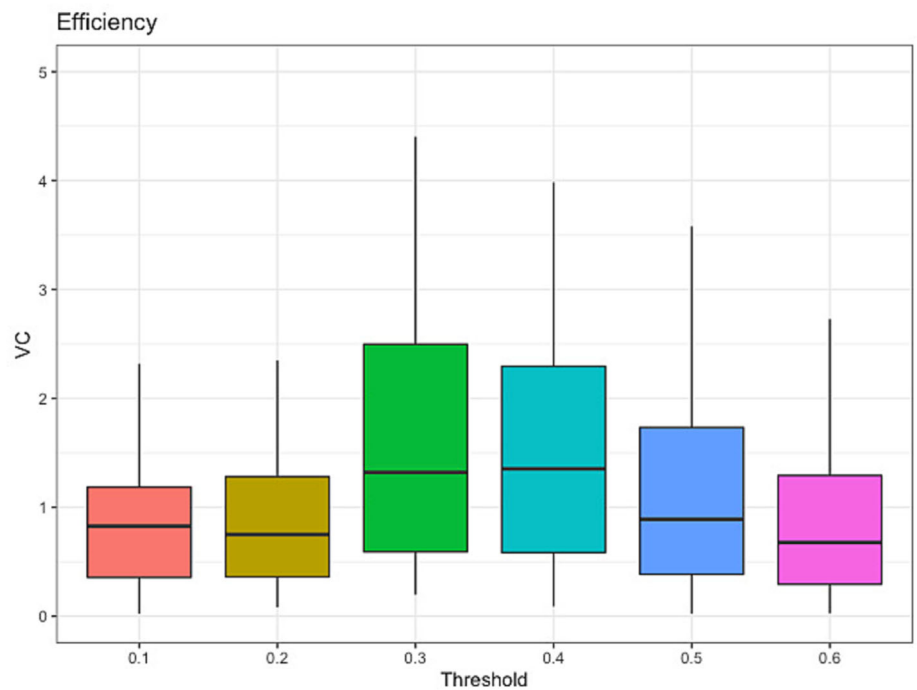


FIGURE 4 Main effect for the coefficient of variation of efficiency depending on threshold. VC, variation coefficient.



($M = 0.89$, $SD = 0.03$). Significant post hoc comparisons for threshold are shown in Table 2.

The results of the mean of efficiency (see Figure 6) showed a significant effect for threshold ($F[5155] = 342.83$; $p < 0.01$) and a significant effect of interaction ($F[5155] = 2.41$; $p = 0.03$). No significant effect for group ($F[1,31] < 1$) was found. Pairwise comparisons over the interaction revealed that for a threshold value of 0.5, the mean in efficiency was significantly lower ($t[89.5] = 2.00$;

$p = 0.04$) for HC ($M = 0.16$, $SD = 0.01$) than for individuals with an SCZ diagnosis ($M = 0.19$, $SD = 0.01$).

3.3 | Relationship with symptom severity

To study the possible relationship between schizophrenia symptom severity and graph measures, we calculated

Spearman's correlation coefficient between PANSS subscales and the measures of integration and segregation. In addition, we included the chlorpromazine equivalent dose and the age of the patients. The results are presented in Table 3.

As can be seen in the table above, no significant relationships were found between network measures and symptomatology. These results are in line with those obtained by other authors (Lynall et al., 2010; Shon et al., 2018), who also found no significant relationship between symptom severity and modularity or efficiency.

4 | DISCUSSION

The healthy human brain operates in a permanent dynamic of segregation and integration of information from internal and external sources. This capacity for dynamic integration–segregation can be considered an evolutionary success, necessary for survival in an ever-

changing environment (Deco et al., 2015). The course of certain mental illnesses, however, could affect this dynamic. In this sense, it has been proposed that SCZ could be related to an imbalance in the information integration–segregation dynamics (Friston & Frith, 1995). Specifically, DMN functioning has been found to be abnormal in schizophrenia (Hu et al., 2017).

On the other hand, research on brain organization based on the resting state has largely ignored the potential for temporal variability, implicitly assuming that the relationships between and within the different brain networks are stationary across the duration of the recordings (Allen et al., 2014). However, some research that has

TABLE 1 Significant post hoc comparisons for the mean of efficiency depending on threshold.

| Contrast | df | t ratio | p value |
|----------|-----|---------|---------|
| 0.1–0.3 | 166 | −3.39 | <0.01 |
| 0.1–0.4 | 166 | −2.95 | <0.01 |
| 0.2–0.3 | 166 | −2.32 | 0.02 |
| 0.3–0.6 | 166 | 2.84 | <0.01 |
| 0.4–0.6 | 166 | 2.41 | 0.01 |

TABLE 2 Significant post hoc comparisons for the mean of modularity depending on threshold.

| Contrast | df | t ratio | p value |
|----------|-----|---------|---------|
| 0.1–0.4 | 166 | −2.71 | 0.01 |
| 0.1–0.5 | 166 | −5.72 | <0.01 |
| 0.1–0.6 | 166 | −8.92 | <0.01 |
| 0.2–0.4 | 166 | −2.75 | <0.01 |
| 0.2–0.5 | 166 | −5.76 | <0.01 |
| 0.2–0.6 | 166 | −8.96 | <0.01 |
| 0.3–0.5 | 166 | −4.71 | <0.01 |
| 0.3–0.6 | 166 | −7.91 | <0.01 |
| 0.4–0.5 | 166 | −3.00 | <0.01 |
| 0.4–0.6 | 166 | −6.20 | <0.01 |
| 0.5–0.6 | 166 | −3.20 | <0.01 |

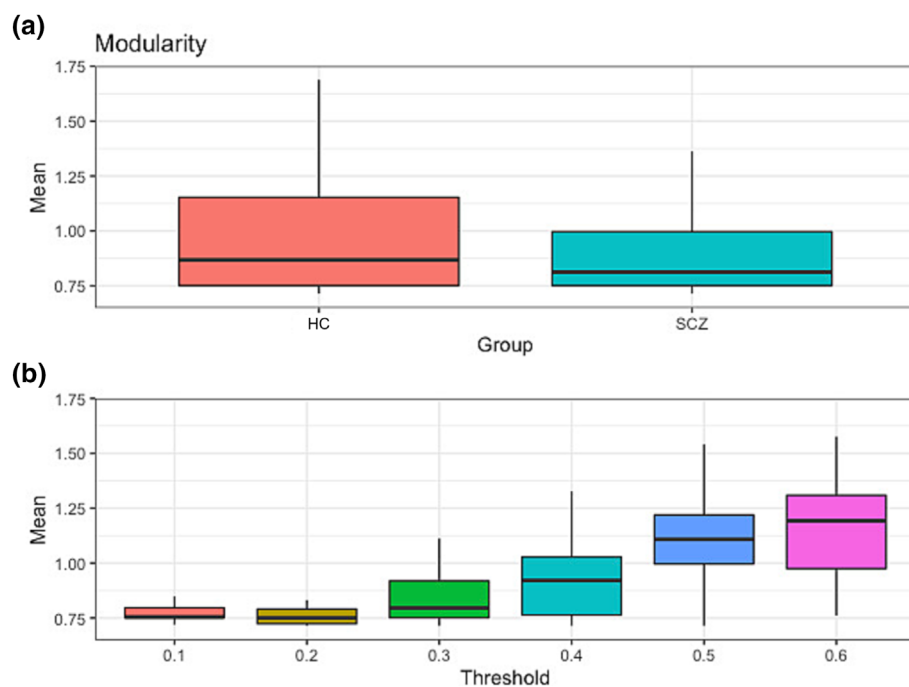


FIGURE 5 Significant Main effects for the mean of modularity depending on group and threshold. (a) Main effect of group. (b) Main effect of threshold. SCZ, schizophrenia.

FIGURE 6 Significant main effects and interaction for the mean of efficiency depending on group and threshold. (a) Interaction group by threshold. (b) Main effect of threshold. SCZ, schizophrenia.

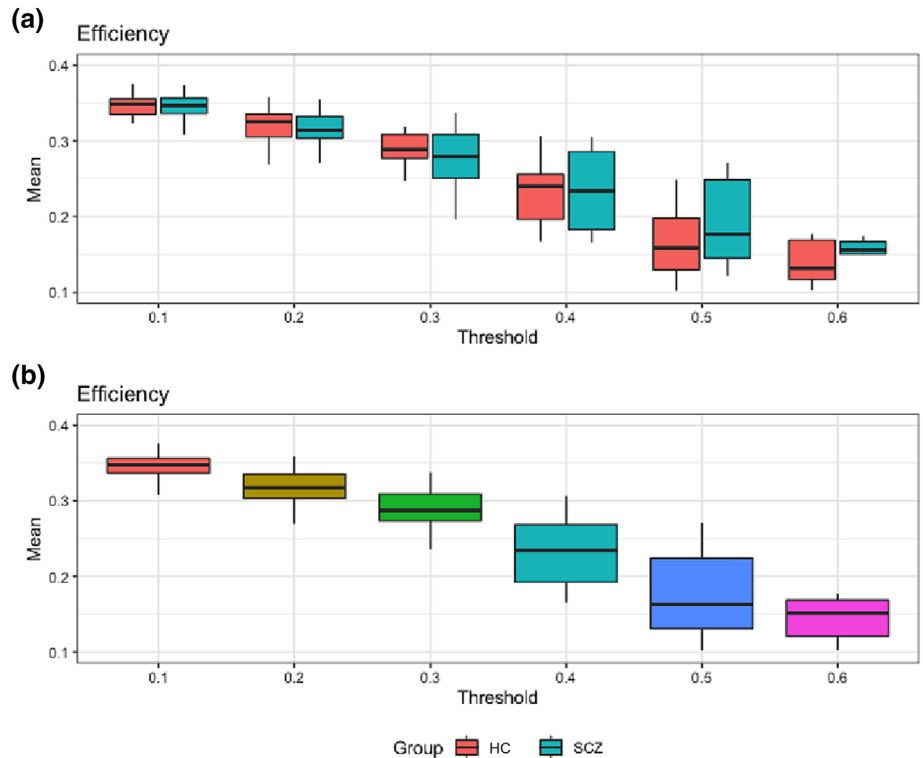


TABLE 3 Correlation coefficients and *p* values (between brackets) for PANSS, dynamical and stationary measures of modularity and efficiency, age of participants and medication (CPZ).

| | PANSS P | PANSS N | PANSS G | Modularity M | Modularity VC | Efficiency M | Efficiency VC | CPZ |
|---------------|----------------------|---------------------|--------------|--------------|----------------------|----------------------|----------------------|-------------|
| PANSS N | 0.43 (0.18) | | | | | | | |
| PANSS G | 0.79* (< .01) | 0.74* (0.01) | | | | | | |
| Modularity M | -0.27 (0.43) | 0.25 (0.47) | 0.01 (0.98) | | | | | |
| Modularity VC | 0.21 (0.52) | -0.26 (0.43) | -0.20 (0.55) | -0.57 (0.07) | | | | |
| Efficiency M | 0.36 (0.26) | 0.21 (0.53) | 0.48 (0.14) | 0.22 (0.52) | -0.71* (0.02) | | | |
| Efficiency VC | 0.33 (0.31) | 0.05 (0.89) | 0.48 (0.14) | 0.17 (0.61) | -0.62* (0.05) | 0.90* (< .01) | | |
| CPZ | 0.39 (0.23) | 0.44 (0.18) | 0.36 (0.28) | -0.08 (0.82) | 0.42 (0.21) | -0.30 (0.37) | -0.30 (0.38) | |
| Age | -0.28 (0.41) | 0.31 (0.36) | -0.17 (0.63) | -0.16 (0.65) | 0.36 (0.27) | -0.70* (0.02) | -0.72* (0.02) | 0.51 (0.11) |

Abbreviations: CPZ, chlorpromazine equivalent; Modularity and Efficiency M, mean measures of modularity and efficiency; Modularity and Efficiency VC: variation coefficient measures of modularity and efficiency; PANSS, Positive and Negative Syndrome Scale; PANSS G: general psychopathology; PANSS N, negative symptoms; PANSS P, positive symptoms.

explicitly studied resting-state functional connectivity dynamics of the DMN has clearly shown the time-varying nature of connectivity (Chang & Glover, 2010), even in individuals with an SCZ diagnosis (Sakoğlu et al., 2010).

In the present work, we aimed to explore the dynamics of integration–segregation in the DMN of patients and healthy controls. For this purpose, from EEG recordings, we obtained functional networks over time from which we calculated the global efficiency and modularity using different thresholds to binarise the matrices. To study the temporal evolution of these indicators, we calculated the coefficient of variation and compared it depending on

the groups of participants (SCZ and HC), the thresholds (0.1 to 0.6), and the interaction between these factors.

The results we obtained regarding the variability of the modularity, indicate a larger repertoire of states of connectivity in the HC group than in the group of individuals with an SCZ diagnosis, particularly in the adjacency matrices obtained at higher thresholds. These results could suggest altered dynamic performance of brain graphs in individuals with an SCZ diagnosis and are in line with previous work (Alexander-Bloch et al., 2010; Rottschy et al., 2012; Yu et al., 2015) in which also has been found that the connectivity states of HCs

changed more frequently than SCZ-diagnosed individuals. This reduced variability of modularity in the SCZ-diagnosed group could be an indicator of rigidity in the segregation–differentiation dynamic within the DMN, which entails the breakdown of the encapsulation of information between brain subsystems specialized in the performance of different tasks. In other words, the SCZs DMN seems to remain in a relatively static connectivity state, characterized by a reduced modularity, whereas HCs dynamically switch between different connectivity states and are therefore faster in recruiting the necessary for the segregated functions of the brain to be performed (Mears & Pollard, 2016). These findings are consistent with previous work on the ‘subtle randomization’ of brain networks in schizophrenia (Lo et al., 2015).

Regarding the results based on averages, similar to what was obtained with the variability measures, we found higher mean modularity in the functional connectivity-based network for the HC group, although, in this case, regardless of the threshold. Here, again, these results seem in agreement with previous results using stationary measures (Alexander-Bloch et al., 2010; Bassett et al., 2008; Bullmore & Sporns, 2009; Liu et al., 2008; Lynall et al., 2010; Rubinov et al., 2009; Vértes et al., 2012), showing that individuals with an SCZ diagnosis and high-risk relatives exhibit lower modularity than healthy controls.

Modular networks promote metastability, a measure of dynamical flexibility (Wildie & Shanahan, 2012) that allows faster adaptation of the system in response to changing environmental conditions. The loss of modularity would prevent any neural activity from remaining locally encapsulated and would fall between the extremes of ceasing quickly and spreading throughout the entire network (Meunier et al., 2010). From this point of view, our results regarding modularity are also consistent with previous work in which an increase in the complexity of cortical activity has been found in individuals with an SCZ diagnosis (Iglesias-Parro et al., 2020) and are consistent with previous studies pointing to ‘subtle randomization’ of brain networks topology in schizophrenia (Alexander-Bloch et al., 2010; Liu et al., 2008; Lo et al., 2015; Lynall et al., 2010; Vértes et al., 2012).

Segregation is supported by densely connected network communities (i.e., hubs, modules of densely intra-connected nodes that are sparsely inter-connected with nodes in other modules) (Deco et al., 2015), and the reduction in segregation is attributed to the decrease in the strength of short-range connections (Mears & Pollard, 2016). Accordingly, our results regarding modularity may indicate that people with schizophrenia tend to have a profile of the DMN functional connectivity associated with a less hub-dominated configuration.

Hubs are particular brain areas, which are heavily implicated in the integration of information. In the normal organization of brain networks, hub areas show a high degree of clustering, and a high degree of centrality, and it is suggested that they are regions that contribute to information integration. In view of our data, however, it appears that in the patient group, a decreased ‘segregation’ of neural processing with the weakening of short-range connections is observed.

Global efficiency has been proposed as a measure of integration, whereby a high efficiency would indicate a high capacity of the network for parallel information transfer (Alexander-Bloch et al., 2010; Latora & Marchiori, 2001). The results we obtained regarding the dynamic of efficiency showed no differences between groups in the variability of efficiency. Although stationary measures of efficiency indicated a general decrease in this variable as the threshold increases, at high thresholds, efficiency was higher in the SCZ-diagnosed group. These results contrast with the efficiency data published in previous studies (Li et al., 2012; Liu et al., 2008; Su et al., 2015), in which a decrease in overall efficiency was found in individuals with an SCZ diagnosis. However, in all these works, efficiency was not calculated for the DMN specifically but for the whole brain. Moreover, they were based on fMRI data and used metrics that were obtained from averages. In contrast, other studies have found higher efficiency in individuals with an SCZ diagnosis (Alexander-Bloch et al., 2010; Hadley et al., 2016; Lo et al., 2015; Lynall et al., 2010). However, the increase in long-range connectivity has been documented in many other papers (Lo et al., 2015; Xia et al., 2019). A first explanation for these data is that the networks of SCZ-diagnosed individuals are better configured for global communication. Increased long-distance strength (i.e., Increased global efficiency) implies higher wiring costs may cause higher network integration (Mears & Pollard, 2016). However, these results are also compatible with research that has found elevated connectivity in the DMN of patients with schizophrenia, which in turn has been related to the inability of patients to allocate resources away from internal thoughts (mind wandering) and towards external stimuli in order to adaptively perform complex tasks (Iglesias-Parro et al., 2020; Whitfield-Gabrieli & Ford, 2012).

It is worth highlighting the results obtained in Table 3 regarding the negative correlation between overall efficiency and age. Most previous studies on global efficiency have shown a reduction in global efficiency in older adults (Achard & Bullmore, 2007; Chong et al., 2019; but see Geerligs et al., 2015). In general, the idea is that brains maximise cost-efficiency by favoring dense short-range connections and sparse long-range

connections because the latter are more costly (Bullmore & Sporns, 2012). Our results suggest a decrease in long-range connections with age. These connections are more costly but greatly increase the speed of information transfer. Reduced global efficiency with age may involve higher wiring costs and a less efficient information flow among distributed networks of the global brain system (Bullmore & Sporns, 2012). In other words, with age, the efficient transfer of information between networks is impaired, resulting in slower processing because the information exchange involves more steps. This process of loss of global efficiency has been interpreted by some researchers as evidence of the topological marginalization of some brain areas because of the aging process.

Also interesting is the negative correlation observed between the variability of modularity and the variability of global efficiency (see Table 3). The idea of coordination dynamics proposes that the tendency of brain regions to express their specialized functions (segregation and modularity) coexists with tendencies to coordinate globally for multiple functions (integration and efficiency). Thus, dense intra-module connections increase local clustering, facilitating functional specialization within the module, whereas sparse inter-module connections optimize network path length and provide the basis for global information integration and increase overall efficiency. According to (Kashtan & Alon, 2005), changes in modularity may allow the brain to adapt to multiple and distinct selection criteria over time. In this sense, this reduction in modularity in schizophrenia had already been proposed as a neuropsychological theory (David, 1994), implying the breakdown of information encapsulation between specialized brain subsystems to perform different tasks.

Overall, our results from the dynamic and stationary measures seem to indicate that the functional networks of patients are less well configured for segregated information processing, that is, for local communication, than those of healthy controls. However, this pattern is reversed for global communication (i.e., global efficiency). Thus, patients, relative to controls, show functional networks, with higher global efficiency and therefore better configured for global communication. These results are congruent with other schizophrenia resting state studies (Alexander-Bloch et al., 2010; Liu et al., 2008; Lynall et al., 2010). This imbalance between the integration and segregation of information in patient networks is consistent with the hypothesis of randomization of functional network topology in SCZ (Alexander-Bloch et al., 2010; Liu et al., 2008; Lynall et al., 2010; Rubinov et al., 2009). These results are also consistent with a model of schizophrenia in which DMN dysfunction is closely linked to deficits in the maintenance of the

integrated self. Thus, insofar as DMN is intimately related to internally directed or self-related cognition, the observed altered dynamics could explain the lack of integration of inner activity (van der Meer et al., 2013).

4.1 | Limitations

The results of this work should be interpreted considering some limitations. First, the participants in our study were a group of patients from St. Agustin Hospital, but the recruitment was not randomized; therefore, selection bias must be considered. In addition, the sample size was relatively small, and care must be taken in generalizing our results to patients undergoing different treatments. In addition, medication is a potential confounding factor regarding the control group. However, antipsychotic dosage (in chlorpromazine equivalents) was not significantly correlated with any of the network metrics.

Second, graph measures, such as efficiency and modularity, depend on how the networks are defined. We began with EEG data, with a limited spatial resolution (albeit high temporal resolution), and reconstructed the sources without individualised anatomical data, and parcellation of the ROIs was performed using an atlas. Caution should be observed when comparing the results of this study with those of studies that defined the networks using another methodology.

Finally, one of the issues in the analysis of neural networks based on functional connectivity is the replicability of the results obtained, due to the presence of false positive links (Buchanan et al., 2020). These false positives are edges in the network that do not represent true connections. In this sense, a higher proportion of false positive connections results in more random network topology, and the differences between groups could simply reflect different noise levels, rather than genuine topological differences. The most common solution to reduce false positives is to employ thresholding by removing 'weak' connections. One difficulty with thresholding is that, with small densities of links (which occur with high thresholds), it can result in networks that have disconnected nodes. Disconnection of networks can affect the quantitative values of many network metrics. Generally, as network sparsity was increased, network efficiency decreased.

AUTHOR CONTRIBUTIONS

Sergio Iglesias-Parro: Conceptualization; data curation; formal analysis; funding acquisition; investigation; methodology; project administration; resources; software; supervision; validation; visualization; writing—original draft; writing—review and editing.

Juan Ruiz de Miras: Conceptualization; data curation; formal analysis; funding acquisition; investigation; methodology; project administration; resources; software; supervision; validation; visualization; writing—original draft; writing—review and editing. **Maria Felipa Soriano:** Conceptualization; data curation; formal analysis; funding acquisition; investigation; methodology; project administration; resources; software; supervision; validation; visualization; writing—original draft; writing—review and editing. **Antonio J. Ibañez-Molina:** Conceptualization; data curation; formal analysis; funding acquisition; investigation; methodology; project administration; resources; software; supervision; validation; visualization; writing—original draft; writing—review and editing.

ACKNOWLEDGEMENTS

This research was funded by Agencia Estatal de Investigación, AEI, PID2019-105145RB-I00.

CONFLICT OF INTEREST STATEMENT

The authors of this work declare no conflict of interest.

DATA AVAILABILITY STATEMENT

The data used in this work and the scripts to analyze them are stored in Figshare. They are available upon reasoned request.

ORCID

Sergio Iglesias-Parro  <https://orcid.org/0000-0001-9153-8743>

PEER REVIEW

The peer review history for this article is available at <https://www.webofscience.com/api/gateway/wos/peer-review/10.1111/ejn.15970>.

REFERENCES

- Achard, S., & Bullmore, E. (2007). Efficiency and cost of economical brain functional networks. *PLoS Computational Biology*, 3(2), e17. <https://doi.org/10.1371/journal.pcbi.0030017>
- Alexander-Bloch, A., Gogtay, N., Meunier, D., Birn, R., Clasen, L., Lalonde, F., Lenroot, R., Giedd, J., & Bullmore, E. (2010). Disrupted modularity and local connectivity of brain functional networks in childhood-onset schizophrenia. *Frontiers in Systems Neuroscience*, 4, 147. <https://doi.org/10.3389/fnsys.2010.00147>
- Allen, E. A., Damaraju, E., Plis, S. M., Erhardt, E. B., Eichele, T., & Calhoun, V. D. (2014). Tracking whole-brain connectivity dynamics in the resting state. *Cerebral Cortex*, 24(3), 663–676. <https://doi.org/10.1093/cercor/bhs352>
- Bassett, D. S., Bullmore, E., Verchinski, B. A., Mattay, V. S., Weinberger, D. R., & Meyer-Lindenberg, A. (2008). Hierarchical organization of human cortical networks in health and schizophrenia. *The Journal of Neuroscience: the Official Journal of the Society for Neuroscience*, 28(37), 9239–9248. <https://doi.org/10.1523/JNEUROSCI.1929-08.2008>
- Bates, D., Mächler, M., Bolker, B., & Walker, S. (2015). Fitting linear mixed-effects models using lme4. *Journal of Statistical Software*, 67(1 SE-Articles), 1–48.
- Bell, A. J., & Sejnowski, T. J. (1995). An information-maximization approach to blind separation and blind deconvolution. *Neural Computation*, 7(6), 1129–1159. <https://doi.org/10.1162/neco.1995.7.6.1129>
- Benjamini, Y., & Yekutieli, D. (2001). The control of the false discovery rate under dependency. *The Annals of Statistics*, 29(4), 1165–1188. <https://doi.org/10.1214/aos/1013699998>
- Bressler, S. L., & Menon, V. (2010). Large-scale brain networks in cognition: Emerging methods and principles. *Trends in Cognitive Sciences*, 14(6), 277–290. <https://doi.org/10.1016/j.tics.2010.04.004>
- Buchanan, C. R., Bastin, M. E., Ritchie, S. J., Liewald, D. C., Madole, J. W., Tucker-Drob, E. M., Deary, I. J., & Cox, S. R. (2020). The effect of network thresholding and weighting on structural brain networks in the UK Biobank. *NeuroImage*, 211, 116443. <https://doi.org/10.1016/j.neuroimage.2019.116443>
- Buckner, R. L. (2013). The brain's default network: Origins and implications for the study of psychosis. *Dialogues in Clinical Neuroscience*, 15(3), 351–358. <https://doi.org/10.31887/DCNS.2013.15.3/rbuckner>
- Buckner, R. L., Andrews-Hanna, J. R., & Schacter, D. L. (2008). The brain's default network. *Annals of the New York Academy of Sciences*, 1124(1), 1–38. <https://doi.org/10.1196/annals.1440.011>
- Bullmore, E., & Sporns, O. (2009). Complex brain networks: Graph theoretical analysis of structural and functional systems. *Nature Reviews Neuroscience*, 10(3), 186–198. <https://doi.org/10.1038/nrn2575>
- Bullmore, E., & Sporns, O. (2012). The economy of brain network organization. *Nature Reviews Neuroscience*, 13(5), 336–349. <https://doi.org/10.1038/nrn3214>
- Chang, C., & Glover, G. H. (2010). Time-frequency dynamics of resting-state brain connectivity measured with fMRI. *NeuroImage*, 50(1), 81–98. <https://doi.org/10.1016/j.neuroimage.2009.12.011>
- Chong, J. S. X., Ng, K. K., Tandi, J., Wang, C., Poh, J. H., Lo, J. C., Chee, M. W. L., & Zhou, J. H. (2019). Longitudinal changes in the cerebral cortex functional organization of healthy elderly. *Journal of Neuroscience*, 39(28), 5534–5550. <https://doi.org/10.1523/JNEUROSCI.1451-18.2019>
- Corsi, M.-C., Chavez, M., Schwartz, D., George, N., Hugueville, L., Kahn, A. E., Dupont, S., Bassett, D. S., & de Vico Fallani, F. (2020). Functional disconnection of associative cortical areas predicts performance during BCI training. *NeuroImage*, 209, 116500. <https://doi.org/10.1016/j.neuroimage.2019.116500>
- David, A. S. (1994). Dysmodularity: A neurocognitive model for schizophrenia. *Schizophrenia Bulletin*, 20(2), 249–255. <https://doi.org/10.1093/schbul/20.2.249>
- Deco, G., Tononi, G., Boly, M., & Kringelbach, M. L. (2015). Rethinking segregation and integration: Contributions of whole-brain modelling. *Nature Reviews Neuroscience*, 16(7), 430–439. <https://doi.org/10.1038/nrn3963>

- Delorme, A., & Makeig, S. (2004). EEGLAB: An open source toolbox for analysis of single-trial EEG dynamics including independent component analysis. *Journal of Neuroscience Methods*, 134(1), 9–21. <https://doi.org/10.1016/j.jneumeth.2003.10.009>
- Desikan, R. S., Ségonne, F., Fischl, B., Quinn, B. T., Dickerson, B. C., Blacker, D., Buckner, R. L., Dale, A. M., Maguire, R. P., Hyman, B. T., Albert, M. S., & Killiany, R. J. (2006). An automated labeling system for subdividing the human cerebral cortex on MRI scans into gyral based regions of interest. *NeuroImage*, 31(3), 968–980. <https://doi.org/10.1016/j.neuroimage.2006.01.021>
- Fischl, B., van der Kouwe, A., Destrieux, C., Halgren, E., Ségonne, F., Salat, D. H., Busa, E., Seidman, L. J., Goldstein, J., Kennedy, D., Caviness, V., Makris, N., Rosen, B., & Dale, A. M. (2004). Automatically parcellating the human cerebral cortex. *Cerebral Cortex (New York, N.Y.: 1991)*, 14(1), 11–22. <https://doi.org/10.1093/cercor/bhg087>
- Fornito, A., Zalesky, A., & Breakspear, M. (2015). The connectomics of brain disorders. *Nature Reviews. Neuroscience*, 16(3), 159–172. <https://doi.org/10.1038/nrn3901>
- Friston, K. J., & Frith, C. D. (1995). Schizophrenia: A disconnection syndrome? *Clinical Neuroscience (New York, N.Y.)*, 3(2), 89–97. <http://europepmc.org/abstract/MED/7583624>
- Friston, K. J., Tononi, G., Sporns, O., & Edelman, G. M. (1995). Characterising the complexity of neuronal interactions. *Human Brain Mapping*, 3(4), 302–314. <https://doi.org/10.1002/hbm.460030405>
- Geerligs, L., Renken, R. J., Saliassi, E., Maurits, N. M., & Lorist, M. M. (2015). A brain-wide study of age-related changes in functional connectivity. *Cerebral Cortex*, 25(7), 1987–1999. <https://doi.org/10.1093/cercor/bhu012>
- Hadley, J. A., Kraguljac, N. V., White, D. M., van Hoef, L., Tabora, J., & Lahti, A. C. (2016). Change in brain network topology as a function of treatment response in schizophrenia: A longitudinal resting-state fMRI study using graph theory. *NPI Schizophrenia*, 2, 16014. <https://doi.org/10.1038/npijschz.2016.14>
- Hilland, E., Johannessen, C., Jonassen, R., Alnæs, D., Jørgensen, K. N., Barth, C., Andreou, D., Nerland, S., Wortinger, L. A., Smelror, R. E., Wedervang-Resell, K., Bohman, H., Lundberg, M., Westlye, L. T., Andreassen, O. A., Jönsson, E. G., & Agartz, I. (2022). Aberrant default mode connectivity in adolescents with early-onset psychosis: A resting state fMRI study. *NeuroImage: Clinical*, 33, 102881. <https://doi.org/10.1016/j.nicl.2021.102881>
- Hu, M.-L., Zong, X.-F., Mann, J. J., Zheng, J.-J., Liao, Y.-H., Li, Z.-C., He, Y., Chen, X.-G., & Tang, J.-S. (2017). A review of the functional and anatomical default mode network in schizophrenia. *Neuroscience Bulletin*, 33(1), 73–84. <https://doi.org/10.1007/s12264-016-0090-1>
- Iglesias-Parro, S., Soriano, M. F., Prieto, M., Rodríguez, I., Aznarte, J. I., & Ibáñez-Molina, A. J. (2020). Introspective and neurophysiological measures of mind wandering in schizophrenia. *Scientific Reports*, 10(1), 1–12. <https://doi.org/10.1038/s41598-020-61843-0>
- Kashtan, N., & Alon, U. (2005). Spontaneous evolution of modularity and network motifs. *Proceedings of the National Academy of Sciences of the United States of America*, 102(39), 13773–13778. <https://doi.org/10.1073/pnas.0503610102>
- Kay, S. R., Opler, L. A., & Lindenmayer, J. P. (1989). The positive and negative syndrome scale (PANSS): Rationale and standardisation. *The British Journal of Psychiatry*, 7, 59–67. <http://www.ncbi.nlm.nih.gov/pubmed/2619982>
- Kybic, J., Clerc, M., Abboud, T., Faugeras, O., Keriven, R., & Papadopoulos, T. (2005). A common formalism for the integral formulations of the forward EEG problem. *IEEE Transactions on Medical Imaging*, 24(1), 12–28. <https://doi.org/10.1109/tmi.2004.837363>
- Latora, V., & Marchiori, M. (2001). Efficient behavior of small-world networks. *Physical Review Letters*, 87(19), 198701. <https://doi.org/10.1103/PhysRevLett.87.198701>
- Lenth, R. V. (2021). emmeans: Estimated Marginal Means, aka Least-Squares Means. R package version 1.5.4. <https://CRAN.R-project.org/package=emmeans>
- Li, X., Xia, S., Bertisch, H. C., Branch, C. A., & DeLisi, L. E. (2012). Unique topology of language processing brain network: A systems-level biomarker of schizophrenia. *Schizophrenia Research*, 141(2–3), 128–136. <https://doi.org/10.1016/J.SCHRES.2012.07.026>
- Liang, M., Zhou, Y., Jiang, T., Liu, Z., Tian, L., Liu, H., & Hao, Y. (2006). Widespread functional disconnectivity in schizophrenia with resting-state functional magnetic resonance imaging. *Neuroreport*, 17(2), 209–213. <https://doi.org/10.1097/01.wnr.0000198434.06518.b8>
- Liu, H., Kaneko, Y., Ouyang, X., Li, L., Hao, Y., Chen, E. Y. H., Jiang, T., Zhou, Y., & Liu, Z. (2012). Schizophrenic patients and their unaffected siblings share increased resting-state connectivity in the task-negative network but not its anticorrelated task-positive network. *Schizophrenia Bulletin*, 38(2), 285–294. <https://doi.org/10.1093/schbul/sbq074>
- Liu, Y., Liang, M., Zhou, Y., He, Y., Hao, Y., Song, M., Yu, C., Liu, H., Liu, Z., & Jiang, T. (2008). Disrupted small-world networks in schizophrenia. *Brain*, 131(4), 945–961. <https://doi.org/10.1093/brain/awn018>
- Lo, C.-Y. Z., Su, T.-W., Huang, C.-C., Hung, C.-C., Chen, W.-L., Lan, T.-H., Lin, C.-P., & Bullmore, E. T. (2015). Randomization and resilience of brain functional networks as systems-level endophenotypes of schizophrenia. *Proceedings of the National Academy of Sciences of the United States of America*, 112(29), 9123–9128. <https://doi.org/10.1073/pnas.1502052112>
- Lynall, M.-E., Bassett, D. S., Kerwin, R., McKenna, P. J., Kitzbichler, M., Muller, U., & Bullmore, E. (2010). Functional connectivity and brain networks in schizophrenia. *Journal of Neuroscience*, 30(28), 9477–9487. <https://doi.org/10.1523/JNEUROSCI.0333-10.2010>
- Mears, D., & Pollard, H. B. (2016). Network science and the human brain: Using graph theory to understand the brain and one of its hubs, the amygdala, in health and disease. *Journal of Neuroscience Research*, 94(6), 590–605. <https://doi.org/10.1002/jnr.23705>
- Meunier, D., Lambiotte, R., & Bullmore, E. (2010). Modular and hierarchically modular organization of brain networks. *Frontiers in Neuroscience*, 4, 200. <https://doi.org/10.3389/fnins.2010.00200>
- Micheloyannis, S., Pachou, E., Stam, C. J., Breakspear, M., Bitsios, P., Vourkas, M., Erimaki, S., & Zervakis, M. (2006).

- Small-world networks and disturbed functional connectivity in schizophrenia. *Schizophrenia Research*, 87(1–3), 60–66. <https://doi.org/10.1016/J.SCHRES.2006.06.028>
- Murphy, K., & Fox, M. D. (2017). Towards a consensus regarding global signal regression for resting state functional connectivity MRI. *NeuroImage*, 154, 169–173. <https://doi.org/10.1016/j.neuroimage.2016.11.052>
- Newman, M. E. J., & Girvan, M. (2003). Finding and evaluating community structure in networks. *Physical Review E*, 69(2), 026113. <https://doi.org/10.1103/PhysRevE.69.026113>
- Pascual-Marqui, R. D. (2002). Standardized low-resolution brain electromagnetic tomography (sLORETA): Technical details. *Methods and Findings in Experimental and Clinical Pharmacology*, 24(Suppl D), 5–12.
- Peralta, V., & Cuesta, M. J. (1994). Psychometric properties of the Positive and Negative Syndrome Scale (PANSS) in schizophrenia. *Psychiatry Research*, 53(1), 31–40. [https://doi.org/10.1016/0165-1781\(94\)90093-0](https://doi.org/10.1016/0165-1781(94)90093-0)
- Rotarska-Jagiela, A., van de Ven, V., Oertel-Knöchel, V., Uhlhaas, P. J., Vogeley, K., & Linden, D. E. J. (2010). Resting-state functional network correlates of psychotic symptoms in schizophrenia. *Schizophrenia Research*, 117(1), 21–30. <https://doi.org/10.1016/j.schres.2010.01.001>
- Rottschy, C., Langner, R., Dogan, I., Reetz, K., Laird, A. R., Schulz, J. B., Fox, P. T., & Eickhoff, S. B. (2012). Modelling neural correlates of working memory: A coordinate-based meta-analysis. *NeuroImage*, 60(1), 830–846. <https://doi.org/10.1016/j.neuroimage.2011.11.050>
- Rubinov, M., Knock, S. A., Stam, C. J., Micheloyannis, S., Harris, A. W. F., Williams, L. M., & Breakspear, M. (2009). Small-world properties of nonlinear brain activity in schizophrenia. *Human Brain Mapping*, 30(2), 403–416. <https://doi.org/10.1002/hbm.20517>
- Rubinov, M., & Sporns, O. (2010). Complex network measures of brain connectivity: Uses and interpretations. *NeuroImage*, 52(3), 1059–1069. <https://doi.org/10.1016/J.NEUROIMAGE.2009.10.003>
- Sakoğlu, Ü., Pearlson, G. D., Kiehl, K. A., Wang, Y. M., Michael, A. M., & Calhoun, V. D. (2010). A method for evaluating dynamic functional network connectivity and task-modulation: Application to schizophrenia. *Magnetic Resonance Materials in Physics, Biology and Medicine*, 23(6), 351–366. <https://doi.org/10.1007/s10334-010-0197-8>
- Shim, G., Oh, J. S., Jung, W. H., Jang, J. H., Choi, C.-H., Kim, E., Park, H.-Y., Choi, J.-S., Jung, M. H., & Kwon, J. S. (2010). Altered resting-state connectivity in subjects at ultra-high risk for psychosis: An fMRI study. *Behavioral and Brain Functions: BBF*, 6, 58. <https://doi.org/10.1186/1744-9081-6-58>
- Shon, S.-H., Yoon, W., Kim, H., Joo, S. W., Kim, Y., & Lee, J. (2018). Deterioration in global organization of structural brain networks in schizophrenia: A diffusion MRI Tractography study. *Frontiers in Psychiatry*, 9, 272. <https://doi.org/10.3389/fpsy.2018.00272>
- Simon, H. A. (1962). The architecture of complexity. *Proceedings of the American Philosophical Society*, 106(6), 467–482. https://doi.org/10.1007/978-3-642-27922-5_23
- Skudlarski, P., Jagannathan, K., Anderson, K., Stevens, M. C., Calhoun, V. D., Skudlarska, B. A., & Pearlson, G. (2010). Brain connectivity is not only lower but different in schizophrenia: A combined anatomical and functional approach. *Biological Psychiatry*, 68(1), 61–69. <https://doi.org/10.1016/j.biopsych.2010.03.035>
- Sporns, O., & Betzel, R. F. (2016). Modular brain networks. *Annual Review of Psychology*, 67(1), 613–640. <https://doi.org/10.1146/annurev-psych-122414-033634>
- Spreng, R. N., Mar, R. A., & Kim, A. S. N. (2009). The common neural basis of autobiographical memory, prospection, navigation, theory of mind, and the default mode: A quantitative meta-analysis. *Journal of Cognitive Neuroscience*, 21(3), 489–510. <https://doi.org/10.1162/jocn.2008.21029>
- Su, T.-W., Hsu, T.-W., Lin, Y.-C., & Lin, C.-P. (2015). Schizophrenia symptoms and brain network efficiency: A resting-state fMRI study. *Psychiatry Research: Neuroimaging*, 234(2), 208–218. <https://doi.org/10.1016/j.pscychres.2015.09.013>
- Uddin, L. Q., Clare Kelly, A. M., Biswal, B. B., Castellanos, F. X., & Milham, M. P. (2009). Functional connectivity of default mode network components: {correlation}, anticorrelation, and causality. *Human Brain Mapping*, 30(2), 625–637. <https://doi.org/10.1002/hbm.20531>
- van Buuren, M., Vink, M., & Kahn, R. S. (2012). Default-mode network dysfunction and self-referential processing in healthy siblings of schizophrenia patients. *Schizophrenia Research*, 142(1), 237–243. <https://doi.org/10.1016/j.schres.2012.09.017>
- van der Meer, L., de Vos, A. E., Stiekema, A. P. M., Pijnenborg, G. H. M., van Tol, M.-J., Nolen, W. A., David, A. S., & Aleman, A. (2013). Insight in schizophrenia: Involvement of self-reflection networks? *Schizophrenia Bulletin*, 39(6), 1288–1295. <https://doi.org/10.1093/schbul/sbs122>
- Vértes, P. E., Alexander-Bloch, A. F., Gogtay, N., Giedd, J. N., Rapoport, J. L., & Bullmore, E. T. (2012). Simple models of human brain functional networks. *Proceedings of the National Academy of Sciences of the United States of America*, 109(15), 5868–5873. <https://doi.org/10.1073/pnas.1111738109>
- Wang, H., Zeng, L. L., Chen, Y., Yin, H., Tan, Q., & Hu, D. (2015). Evidence of a dissociation pattern in default mode subnetwork functional connectivity in schizophrenia. *Scientific Reports*, 5(May), 1–10. <https://doi.org/10.1038/srep14655>
- Whitfield-Gabrieli, S., & Ford, J. M. (2012). Default mode network activity and connectivity in psychopathology. *Annual Review of Clinical Psychology*, 8(September), 49–76. <https://doi.org/10.1146/annurev-clinpsy-032511-143049>
- Whitfield-Gabrieli, S., Thermenos, H. W., Milanovic, S., Tsuang, M. T., Faraone, S. V., McCarley, R. W., Shenton, M. E., Green, A. I., Nieto-Castanon, A., LaViolette, P., Wojcik, J., Gabrieli, J. D. E., & Seidman, L. J. (2009). Hyperactivity and hyperconnectivity of the default network in schizophrenia and in first-degree relatives of persons with schizophrenia. *Proceedings of the National Academy of Sciences*, 106(4), 1279–1284. <https://doi.org/10.1073/pnas.0809141106>
- Wildie, M., & Shanahan, M. (2012). Metastability and chimera states in modular delay and pulse-coupled oscillator networks. *Chaos (Woodbury, N.Y.)*, 22(4), 43131. <https://doi.org/10.1063/1.4766592>
- Xia, M., Womer, F. Y., Chang, M., Zhu, Y., Zhou, Q., Edmiston, E. K., Jiang, X., Wei, S., Duan, J., Xu, K., Tang, Y., He, Y., & Wang, F. (2019). Shared and distinct functional

- architectures of brain networks across psychiatric disorders. *Schizophrenia Bulletin*, 45(2), 450–463. <https://doi.org/10.1093/schbul/sby046>
- Yu, Q., Erhardt, E. B., Sui, J., Du, Y., He, H., Hjelm, D., Cetin, M. S., Rachakonda, S., Miller, R. L., Pearlson, G., & Calhoun, V. D. (2015). Assessing dynamic brain graphs of time-varying connectivity in fMRI data: Application to healthy controls and patients with schizophrenia. *NeuroImage*, 107, 345–355. <https://doi.org/10.1016/j.neuroimage.2014.12.020>
- Zhou, L., Pu, W., Wang, J., Liu, H., Wu, G., Liu, C., Mwansisya, T. E., Tao, H., Chen, X., Huang, X., Lv, D., Xue, Z., Shan, B., & Liu, Z. (2016). Inefficient DMN suppression in schizophrenia patients with impaired cognitive function but not patients with preserved cognitive function. *Scientific Reports*, 6, 21657. <https://doi.org/10.1038/srep21657>
- Zhou, Y., Liang, M., Jiang, T., Tian, L., Liu, Y., Liu, Z., Liu, H., & Kuang, F. (2007). Functional dysconnectivity of the dorsolateral prefrontal cortex in first-episode schizophrenia using resting-state fMRI. *Neuroscience Letters*, 417(3), 297–302. <https://doi.org/10.1016/j.neulet.2007.02.081>

How to cite this article: Iglesias-Parro, S., Ruiz de Miras, J., Soriano, M. F., & Ibáñez-Molina, A. J. (2023). Integration–segregation dynamics in functional networks of individuals diagnosed with schizophrenia. *European Journal of Neuroscience*, 1–15. <https://doi.org/10.1111/ejn.15970>